

Invited Review Article: The electrostatic plasma lens

Cite as: Rev. Sci. Instrum. **84**, 021101 (2013); <https://doi.org/10.1063/1.4789314>

Submitted: 17 July 2012 . Accepted: 04 November 2012 . Published Online: 05 February 2013

Alexey Goncharov



View Online



Export Citation



CrossMark

ARTICLES YOU MAY BE INTERESTED IN

[Electrostatic plasma lens for focusing negatively charged particle beams](#)




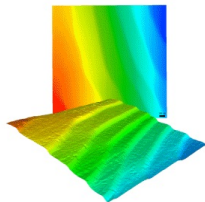
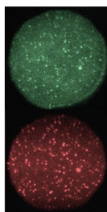
Review of Scientific Instruments **83**, 02B723 (2012); <https://doi.org/10.1063/1.3675387>

[Recent development of plasma optical systems \(invited\)](#)

Review of Scientific Instruments **87**, 02B901 (2016); <https://doi.org/10.1063/1.4931718>

[Focusing of high-current, large-area, heavy-ion beams with an electrostatic plasma lens](#)

Applied Physics Letters **75**, 911 (1999); <https://doi.org/10.1063/1.124551>

 <p>MCL MAD CITY LABS INC. www.madcitylabs.com</p>	<p>Nanopositioning Systems</p> 	<p>Modular Motion Control</p> 	<p>AFM and NSOM Instruments</p> 	<p>Single Molecule Microscopes</p> 
---	--	--	---	--

Invited Review Article: The electrostatic plasma lens

Alexey Goncharov^{a)}

Institute of Physics, National Academy of Sciences of Ukraine, Kiev 680028, Ukraine

(Received 17 July 2012; accepted 4 November 2012; published online 5 February 2013)

The fundamental principles, experimental results, and potential applications of the electrostatic plasma lens for focusing and manipulating high-current, energetic, heavy ion beams are reviewed. First described almost 50 years ago, this optical beam device provides space charge neutralization of the ion beam within the lens volume, and thus provides an effective and unique tool for focusing high current beams where a high degree of neutralization is essential to prevent beam blow-up. Short and long lenses have been explored, and a lens in which the magnetic field is provided by rare-earth permanent magnets has been demonstrated. Applications include the use of this kind of optical tool for laboratory ion beam manipulation, high dose ion implantation, heavy ion accelerator injection, in heavy ion fusion, and other high technology. © 2013 American Institute of Physics. [<http://dx.doi.org/10.1063/1.4789314>]

I. INTRODUCTION

High-current ion beams are used widely for basic research and high-technology applications, including for example, in heavy ion fusion research, high current linear accelerators, spacecraft control systems, high dose ion implantation for material surface modification, and for surface cleaning and activation prior to film deposition. The manipulation (focusing, beam profile control, bending) of ion beams is well understood for the case of low current beams where space charge compensation of the beam is not required. But when the ion beam current is high and a high degree of space charge neutralization by a background sea of cold electrons is required in order for the beam to propagate and not to be lost to space charge blow-up, there exists a significant lack of tools for manipulating the beam in any way. There is thus a need for an alternative to traditional vacuum ion optic systems (electrostatic and magnetic lenses) for the case of high-current ion beams.

A “pure” ion beam, meaning here an energetic beam of positive ions propagating in vacuum in the absence of any other charged particles, electrons in particular, assumes a potential that can be very high due to the positive ion charge of the beam itself. This high space charge can lead to the growth of the beam cross-section due to radial motion of the ions under the influence of the electric field set up by the positive ion space charge. This is referred to as space charge blow-up and can lead to degradation of the beam current density and loss of beam via scrape-off of the outer beam regions. Although it is not uncommon for ion beam space charge considerations to be simply ignored, these concerns are important and often critical, especially for high current heavy ion beams. In order to prevent space charge blowup of the beam, charge-compensating particles, i.e., cold electrons (for the case of a positive ion beam), need to be introduced to the interior beam volume. There are in general a number of possible sources of cold electrons or mechanisms by which electrons can be introduced into the beam in order to provide space charge neu-

tralization (also called space charge compensation). The collision of energetic beam ions with residual gas atoms in the downstream volume is one obvious such source. For the case of a gaseous ion source, neutrals enter the beam volume primarily from the ion source itself, and the neutral gas density is highest close to the beam extractor. Energetic positive ions can suffer charge exchange collisions with neutral gas atoms (charge exchange has the highest cross section), resulting in fast neutral atoms and slow thermal ions. The secondary thermal ions experience the electric field of the uncompensated ion beam and are accelerated toward the chamber wall, where they generate secondary electrons that are in turn attracted back to the positive beam region. This two-stage process can in many cases be the primary source of charge-compensating electrons. Another source of cold electrons is the direct ionizing collision of fast beam ions with background neutrals, which produces slow positive ions that are ejected from the beam by the beam space charge forces and cold electrons that remain within the beam and build up in density. Yet another source can be scrape-off electrons produced by the secondary emission of electrons from the ground grid (the final extractor electrode, which is at ground potential) of the beam formation electrode configuration via grazing collisions of energetic beam ions with the metal electrode. Finally, another source can be secondary electrons produced by beam ions striking the target and/or grounded vessel. There are thus many possible ways in which the beam can rapidly acquire its background sea of cold electrons, and one reason why the concern of beam space charge is often ignored is because beam neutralization is very often “automatic” — the experiment or application suffers no ill-effects because the overlooked space charge neutralization is spontaneously provided by the set-up itself.

When an energetic ion beam is passed through a beam focusing device, however, the concern of space charge neutralization increases in importance. The Einzel lens, in particular, is completely inappropriate for use with high current beams, as the lens electric field severely impedes the flow of cold electrons within the beam and beam neutralization fails. What is observed experimentally is that the ion beam, rather

^{a)}Electronic mail: gonchar@iop.kiev.ua.

than being focused by the Einzel lens, is in fact “defocused” (it “blows up”) due to beam expansion under its own radial ion space charge forces. Said otherwise, the Einzel lens is a tool that is appropriate for the case of low current ion beams when the beam can propagate without the need for space charge neutralization, but it is inappropriate for use with high current beams. The situation for magnetic lenses is more complicated, since space charge neutralization can in some cases be preserved to some extent. It is clear, however, that there would be great advantage in a beam focusing device that maintains full beam neutralization even for high current beams under all circumstances. This is the niche filled by the plasma lens.

The term “high current” is used here to mean that space charge forces are significant and that neutralization of the beam space charge by cold electrons (for a positive ion beam) is necessary in order for the beam to propagate without blow-up. Ion beams of this kind can be viewed as a quasi-neutral plasma medium containing fast ions and cold electrons. The beam potential parameter, I_b/v_b , is the potential drop from center to edge of an uncompensated cylindrical ion beam propagating with total current I_b and beam velocity v_b . For illustration consider a singly charged copper ion beam with current 1 A and energy 10 keV; the beam potential parameter for this case is about 50 keV. Clearly, this huge potential, due to the uncompensated beam space charge, can lead to extreme growth of the beam cross-section. The propagation of high current ion beams has been studied by a number of authors, perhaps initiated by the beam blow-up problems experienced with the “Calutron” mass-separation of intense ion beams.¹ A review and summary of partially compensated beam transport has been presented by Holmes.² The radial expansion (“blow-up”) of an ion beam due to uncompensated space charge is very often not a small effect, even though it is often ignored without detriment as described above because of the automatic space charge compensation that is frequently provided by the system itself. For example, it can be readily shown from Holmes² that a 1 mm diameter beam of 10 keV hydrogen ions of current 10 mA will double its initial radius in a distance of just 1 cm. The important point is that space charge blow-up concerns are very often not negligible, especially so for ion beam focusing devices. The plasma lens is important in this way.

There has been in recent years heightened interest in experimental heavy ion fusion research, due in part to progress in the development of solid state ion sources (alumino silicate sources) for providing intense, high brightness, heavy alkali metal ion beams. High energy density as required for fusion application calls for simultaneous compression of the beam pulse both in the longitudinal and transverse directions. Thus the intense ion beam must be substantially compressed radially by passage through a focusing device. The electrostatic plasma lens has the high optical strength for focusing intense quasi-neutral ion beams and can provide a unique tool for these important applications.

II. BACKGROUND AND OVERVIEW

The electrostatic plasma lens is an axially symmetric plasma-optics device with a set of cylindrical ring electrodes

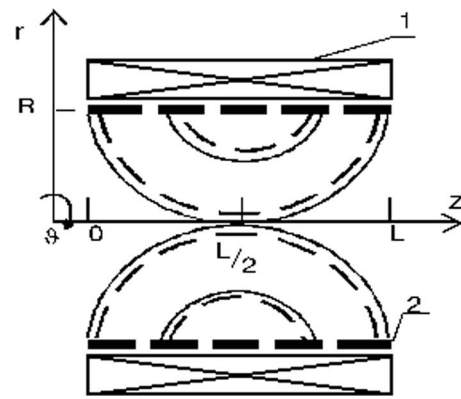


FIG. 1. Schematic of plasma lens. 1 – magnetic field coils; 2 – cylindrical electrodes. Dashed lines – equipotentials. Solid lines – magnetic field lines. Reprinted with permission from A. A. Goncharov and I. G. Brown, *IEEE Trans. Plasma Sci.* **32**, 80 (2004). Copyright 2004 Institute of Electrical and Electronics Engineers, Inc.

located within the magnetic field region, with magnetic field lines connecting ring electrode pairs symmetrically about the lens midplane; see Fig. 1. This is quite different from the magnetostatic plasma lens, where charged particle focusing is provided by the azimuthal magnetic field established in a cylindrical plasma column by a powerful axial discharge of current typically $\sim 10^3 - 10^6$ A, leading to a focal length F that varies as $\sim (v_b/I_d)^{1/2}$, where I_d is the discharge current and v_b is the beam ion velocity. Panofsky and Baker³ provided the first demonstration of this kind of magnetostatic lens, successfully focusing energetic (up to 350 MeV) short-pulse proton beams after passage through an accelerator. The approach was developed theoretically by a number of workers,⁴⁻⁶ and the possibility of using the method for focusing relatively long-pulse (600 μ s), moderate energy ion beams was recognized.⁷ These experiments achieved a compression factor of the focused beam of up to 500.

The basic concept of the electrostatic plasma lens was first described by Morozov and co-workers,⁸⁻¹⁰ and is based on the use of magnetically insulated cold electrons (i.e., transverse mobility \ll parallel mobility) to provide space-charge neutralization of the focused ion beam and maintain the magnetic field lines as equipotentials (“equipotentialization”). These early contributions also clarified the advantages of plasma lenses as compared with the more traditional electrostatic lens (of which the Einzel lens is one specific kind) and magnetic lenses (see Refs. 9 and 10 for detail). This is a generalization of Gabor’s ideas for employing a magnetized electron cloud in a Penning trap as an effective space charge lens for focusing low current positive ion beams.¹¹ Recent years have witnessed increased application of Gabor type lenses in low energy beam lines for focusing light ions such as of He^+ .^{12,13} An example of a simplified classical Gabor lens is shown schematically in Fig. 2. This kind of lens is attractive for focusing narrow single-aperture, low-current ion beams.

Electrons within the electrostatic plasma lens volume can be formed by many different methods, for example, by secondary electron emission from collision of beam ions with the lens electrodes, and are able to stream freely along the magnetic field lines, thereby tying the potential to that of the

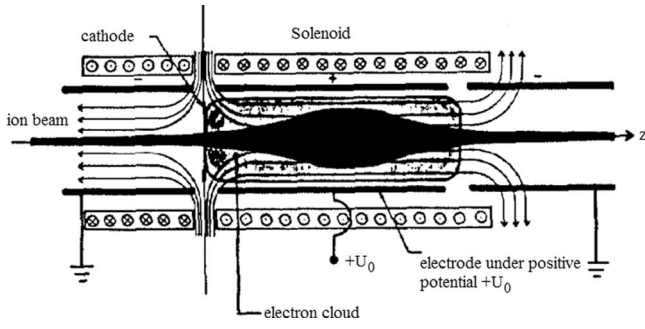


FIG. 2. Simplified schematic of Gabor space charge lens. Reprinted with permission from D. Gabor, *Nature (London)* **160**, 89 (1947). Copyright 1947 Macmillan.

electrostatic ring electrode to which the field line is attached. This method of generation of the needed electrons is convenient for wide-aperture, high-current, pulsed heavy ion beams. A steady state is rapidly reached on the time-scale of the electron flow along magnetic field lines (i.e., approximately the electron time of flight), and preserved because of the closed azimuthal drift of electrons in the $\mathbf{E} \times \mathbf{B}$ field of the lens. The condition of equipotential magnetic field lines of length $l \gg R$, the lens radius, passing through the axial region of the system and crossing the outermost electrodes (which are grounded) follows from a model in which the lens volume is uniformly filled with cold background electrons of density n_e and energetic beam ions of density $n_b = I_b / (eQv_b\pi R^2)$, where eQ is the ion charge, with e the electronic charge and Q the ion charge state (1, 2, 3, ...), v_b the beam ion velocity, and R the beam radius. This condition can be given as^{14,15}

$$n_e - \frac{I_b}{eQv_b\pi R^2} = \pm \frac{\varphi_L}{e\pi R^2}, \quad (1)$$

where φ_L is the maximum electric potential on the ring electrodes. The plus sign corresponds to beam focusing and the minus sign to beam defocusing – the dispersive operational regime of the lens.¹⁴ Here, we assume Q to be the mean ion charge state, for simplicity. However, as for all purely electrostatic charged-particle optical systems, the focusing characteristics of the electrostatic plasma lens are charge-state-independent, noting that the function of the lens magnetic field is to tie electrons to field lines, and neglecting for now the small azimuthal $\mathbf{v}_{ion} \times \mathbf{B}_{lens}$ force. (See later, however, our discussion about momentum aberrations). In order that equipotential magnetic field lines be generated, an electron density is needed that is sufficient to compensate both the space charge due to the beam and the vacuum electric potential within the lens volume. It can be seen from Eq. (1) that beam focusing can be obtained for low ion beam density – this is similar to the Gabor lens. In this case, the ion beam density does not play a role and the electrons are used only for space charge compensation and transformation of the external vacuum electric field in order to make the electric field lines transverse to the magnetic field lines for focusing low current positive ion beams.

For a high current beam when, if unneutralized, the beam could blow up under its own space-charge forces, neutralization can be provided by electrons of sufficient density held

within the beam by its space charge. This regime occurs when the beam potential parameter I_b/v_b exceeds significantly the maximum externally applied lens voltage, $I_b/v_b \gg \varphi_L$. This operational regime of the high-current plasma lens has been reported by us previously.^{16,17} In the high beam current regime, a quasi-neutral plasma is formed within the lens volume consisting of cold magnetized electrons drifting along the magnetic field lines and fast beam ions that are affected to first approximation only by the radial electrostatic field of the lens. Note that the equipotentialization condition follows from the steady-state hydrodynamic equation of motion of cold electrons, which in this case is^{8–10}

$$\mathbf{E} = -1/c(\mathbf{v}_d \times \mathbf{B}), \quad (2)$$

where \mathbf{v}_d is the velocity of cold electrons, \mathbf{B} is the magnetic field within the lens volume, and c is the velocity of light. The macroscopic electrostatic field \mathbf{E} can exist only in the presence of closed electron drift and an “insulating” magnetic field. Then the electric field is perpendicular to the magnetic field, leading to magnetic field lines that are equipotentials. It follows that the self-consistent potential distribution within the lens volume depends on the magnetic field as

$$\Phi = k\Psi(r, z), \quad (3)$$

where k is a proportionality coefficient determined by the boundary conditions. Here, Ψ is the magnetic flow function related to the magnetic field by

$$B_r = -\frac{1}{r} \frac{\partial \Psi}{\partial z}, \quad B_z = \frac{1}{r} \frac{\partial \Psi}{\partial r}. \quad (4)$$

The lines $\Psi = \text{const.}$ are magnetic field lines. It is also necessary that the magnetic field configuration should eliminate spherical aberrations and transfer ground potential (the potential of the outermost lens electrodes) to the beam axis at the midplane. We note parenthetically that by the term spherical aberration we follow conventional usage and that of Morozov,^{9,10} and refer to the case when the radial electric field $E_r(r)$ has a variation other than linear; when $E_r(r) \sim r$, there are no spherical aberrations, and a zero-divergence, mono-energetic ion beam can be brought to a perfect focus. For this case, we can write

$$\Phi \sim \Psi = \frac{B(0, z)}{2} r^2 - \frac{B''(0, z)}{16} r^4 + \dots, \quad (5)$$

where to good approximation the correction for the second term proportional to r^4 is small (for more detail see Ref. 9). One can also see that it is necessary to choose an optimized magnetic field configuration in order to eliminate spherical aberrations. (See latter discussion about advanced plasma lenses with minimized magnetic field gradients).

The focal length F of this kind of electrostatic plasma lens is given by^{9,10}

$$F = \frac{\theta \varphi_b R}{2\varphi_L}, \quad (6)$$

where φ_b is the ion beam accelerating potential (i.e., φ_b is the ion source extractor voltage and the energy of the beam ions is $E_b = eQ\varphi_b$), φ_L is the maximum electric potential on the ring electrodes, and θ is a geometric parameter that depends on the ratio of lens radius R to lens length L and the magnetic

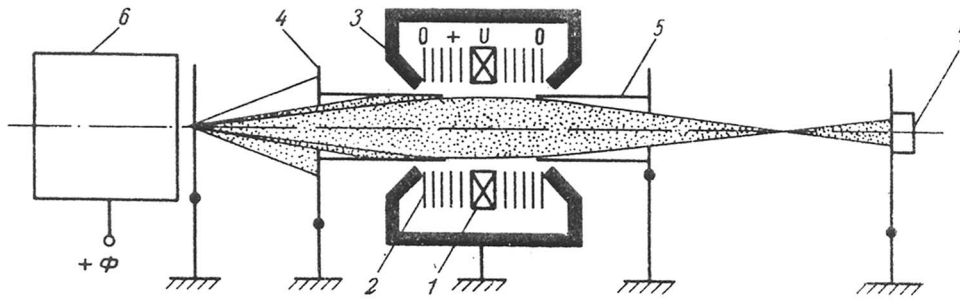


FIG. 3. Experimental setup for the first investigation of the electrostatic plasma lens. 1 – magnetic field coil; 2 – fixing electrodes; 3 – magnetic core; 4 and 5 – electron compensators (by secondary electron emission); 6 – plasma ion source; 7 – collector. Reprinted with permission from JETP Lett. **9**(1), 24 (1969). Copyright 1969 American Institute of Physics.

field configuration. For the optimal configuration, $\theta \approx 1$; the optimal configuration of magnetic field has been shown¹⁶ to occur for $\theta = (\pi R/L)I_1(1)$, where I_1 is the modified Bessel function. Importantly, note that the focal length of the plasma lens does not depend on the ion charge-to-mass ratio; this is a consequence of the purely electrostatic optical system, as previously mentioned.

Electrostatic plasma lenses have been investigated for half a century. This background work is characterized by a steady increase in the ion beam current I_b and the beam potential parameter I_b/v_b . Experiments demonstrating the potential of the plasma optical concept for focusing ion beams were described initially in Ref. 18, following which the plasma optical approach was developed¹⁹ at the Institute of Physics, NASU, at Kiev, using a range of plasma lens geometries for focusing intense ion beams.

The first electrostatic plasma lens experiments were carried out at Morozov's initiative at the Kurchatov Institute, Moscow, in the late-1960s,^{9,18} see Fig. 3. The ion source provided a steady-state beam of Ar or He ions with current 0.5–15 mA at the entrance to the plasma lens and with energy up to 10 keV. The residual pressure within the vacuum chamber was about 1×10^{-5} Torr. Secondary electron emission was used for creation of the plasma medium within the lens volume. Knowing the distances (a) from the ion source exit to the midplane of the lens, and (b) from midplane to focus, the focal length, f_e , of the plasma lens for given experimental conditions was determined using the well-known formula for a thin lens $1/f = 1/f_a + 1/f_b$. Figure 4 shows the ratio of the ex-

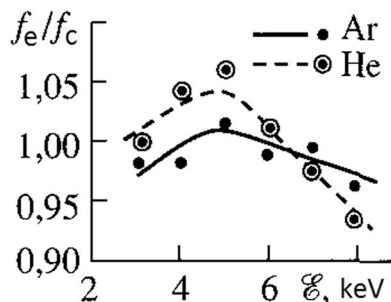


FIG. 4. Dependence of the ratio of experimental focal length f_e to calculated f_c on ion beam energy. From Morozov, *Encyclopedia of Low-Temperature Plasma*. Copyright 2008 by Springer. Reprinted with permission of Springer.

perimental focal length (f_e) to that calculated (f_c) from Eq. (6) for the same conditions. We see also (Fig. 5) that decreasing the magnetic field strength within the lens volume destroys the plasma medium due to elimination of electron magnetic isolation and leads to only a weak lens optical strength.

These experiments were the first to point out the attractive and extensive possibilities of the introduction of the plasma optical principles of macroscopic electrostatic fields in the plasma medium as being suitable for focusing intense positive ion beams. Note also that these experiments demonstrated explicitly that the optical strength of the plasma lens can be up to two orders of magnitude greater than for an Einzel lens and up to four orders of magnitude greater than for a magnetic lens, under the same experimental conditions. In other words, achieving the same focusing would require much greater lens electric or magnetic field strength.

III. LOW-CURRENT PLASMA LENS

A. Short electrostatic plasma lens

A schematic of the setup used for investigation of focused ion beams using a short plasma lens is shown in Fig. 6.¹⁹ Steady-state beams of helium ions with energy up to 35 keV and current up to 40 mA were formed by a duoplasmatron ion source with a single-aperture extractor of diameter 4 mm by means of an optimized quasi-Pierce system 1, which enabled limiting the divergence of the ion beam at the lens entrance. The plasma lens aperture formed by nine mutually isolated tantalum cylindrical electrodes 2 was 26 mm, and the length of the lens was 66 mm. The magnetic field (500–1000 G on-axis) was formed by the current-driven field

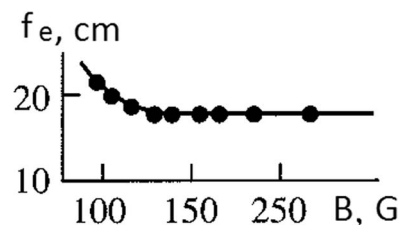


FIG. 5. Dependence of measured focal length f_e on magnetic field strength. From Morozov, *Encyclopedia of Low-Temperature Plasma*. Copyright 2008 by Springer. Reprinted with permission of Springer.

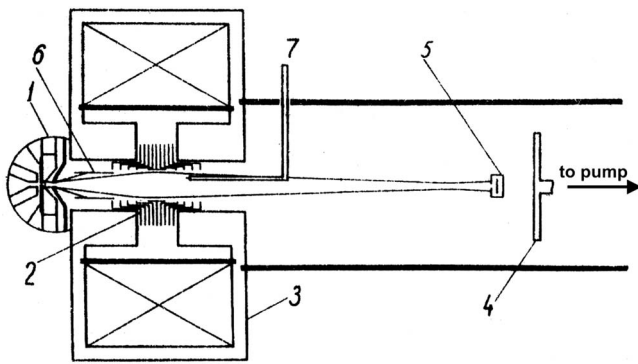


FIG. 6. Experimental set up for short plasma lens. 1 – ion source and quasipierce optical system; 2 – plasma lens; 3 – magnetic system; 4 – ion collector; 5 – diaphragm; 6 – electron compensator; 7 – Langmuir probe. From M. Gabovich, I. Gasanov, and I. Protsenko, *Plasma Lenses for Formation of Ion Beams* (Institute of Physics AS USSR, Kiev, 1982), Preprint # 8. Copyright 1982 by Institute of Physics NAS of Ukraine. Reprinted with permission of Institute of Physics NAS of Ukraine.

coils 3 and was localized by pole pieces to the gap between them. The potential distribution of the electrodes was varied so as to obtain optimum focusing; the central electrode was held at a potential of up to 4 kV. Electron injection into the lens volume was by secondary electron emission from the walls of the electron compensator tube 6, of 18 mm internal diameter, which was held at ground potential. Note that beam focusing was not observed when the compensator was removed. Maximum observed ion beam current density at the focus was up to about 300 mA/cm². Beam current was measured by collector 4 using both electric and calorimetric methods. For determining the beam current density, diaphragm 5 with a 0.5 mm hole moveable in the radial direction was located in front of the collector. The electric potential value and configuration in the lens volume was measured by the isolated Langmuir probe 7, and the characteristics of the magnetic field were measured by magnetic probes. Residual gas pressure in the vacuum chamber was 3×10^{-6} Torr.

B. Self-consistent mode

The dependence of current density at the focus on the total beam current is shown in Fig. 7, which demonstrates the lens action over this range of current. In addition, studies of a “self-consistent” lens operation mode were carried out without supplying external voltage to the ring electrodes. It was determined that in this case the value and distribution of steady-state electrode potential depends on the electrode geometry and “accessibility” to ions at the beam boundary. Measurements of the radial distribution of current density at the focus (Fig. 8) revealed that the lens focusing properties in this “self-consistent” mode (lower curve in the figure) are somewhat superior to that of the “conventional” case.

The focusing of intense diverging ion beams formed by an ion source at only a short distance (about 7 cm) from the lens midplane provides evidence of a strong radial electric field within the lens. Estimation of the field value from the expression for lens focal length, Eq. (6), using the experimentally determined lens optical strength, shows that practically the entire applied potential difference is distributed radially.

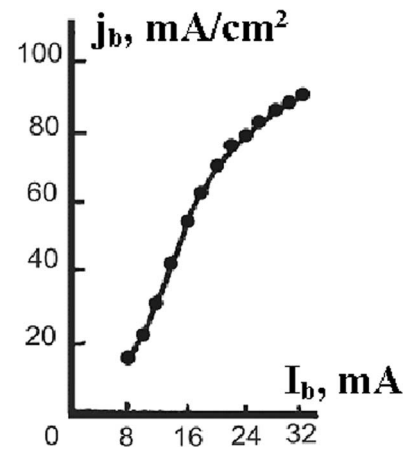


FIG. 7. Dependence of current density at the focus on total beam current. From M. Gabovich, I. Gasanov, and I. Protsenko, *Plasma Lenses for Formation of Ion Beams* (Institute of Physics AS USSR, Kiev, 1982), Preprint # 8. Copyright 1982 by Institute of Physics NAS of Ukraine. Reprinted with permission of Institute of Physics NAS of Ukraine.

For the obtained value of $f = 5-6$ cm, the mean electric field value should be about 3 kV/cm. One can see from the measured radial potential distributions at the lens midplane (Fig. 9) in the “conventional” (upper curve) and “self-consistent” (lower curve) modes, that strong electric fields are indeed formed in the system, in agreement with the estimates given above.

Thus beam focusing without an external supply of voltage to the lens electrodes has been observed.¹⁹ Beam focusing quality in this case was somewhat better than in the “conventional” case. Electrodes acquire their potential by contact with a fraction of the beam periphery. The action of the radial electric field of the ions and the presence of electrons in the system result in a self-consistent distribution of potential across the electrodes. When the electron compensator was moved inside the lens by a small amount, thus causing the electrodes

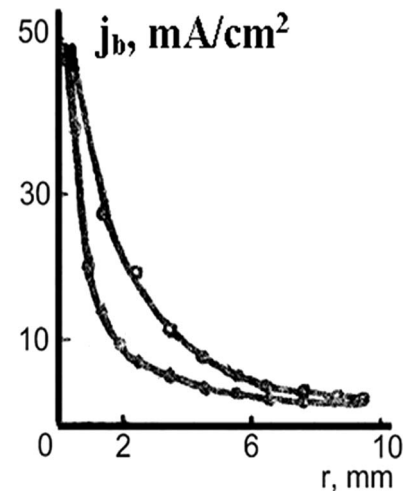


FIG. 8. Radial distribution of ion current density at the beam focus. Upper curve – “conventional” mode; lower curve – “self-consistent” mode. From M. Gabovich, I. Gasanov, and I. Protsenko, *Plasma Lenses for Formation of Ion Beams* (Institute of Physics AS USSR, Kiev, 1982), Preprint # 8. Copyright 1982 by Institute of Physics NAS of Ukraine. Reprinted with permission of Institute of Physics NAS of Ukraine.

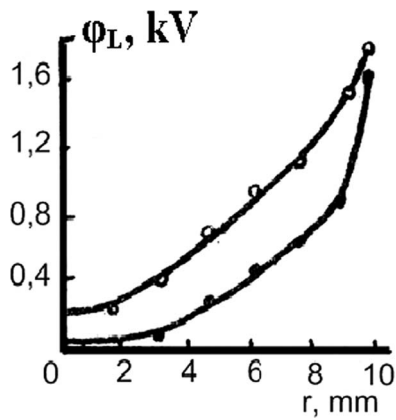


FIG. 9. Radial potential distribution at the lens midplane. Upper curve – “conventional” mode; lower curve – “self-consistent” mode. From M. Gabovich, I. Gasanov, and I. Protsenko, *Plasma Lenses for Formation of Ion Beams* (Institute of Physics AS USSR, Kiev, 1982), Preprint # 8. Copyright 1982 by Institute of Physics NAS of Ukraine. Reprinted with permission of Institute of Physics NAS of Ukraine.

to be inaccessible to fast particles, no potential difference occurred between the electrodes and the beam was not focused. Note that this self-consistent plasma-optical regime has also been observed in passing a low-energy plasma flow through an isolated curvilinear plasma guide used as a separator in the plasma configuration used for pre-cleaning in plasma coating devices.²⁰

Robertson has reported²¹ on the “collective” focusing of intense current-neutralized and charge-neutralized ion beams passed through a dielectric tube in the low magnetic field regime (about 75 G), and theoretical calculations were presented. The experimentally observed focusing is explained by contraction of electron flow moving with the beam velocity. Due to space charge redistribution, a radial electric field is established in such a two-component plasma, leading to focusing of the ions. At the same time, upon replacement of the dielectric drift tube by a metal tube, the focusing effect disappeared. We hypothesize an alternative explanation of the experimental observations. We speculate that it is probable that in this case a self-consistent plasma lens operational mode was realized, in which the central dielectric electrode was charged by the beam, and electrons collisionally ejected from the grounded metal end flanges were acquired within the system. The disappearance of focusing when the dielectric tube was replaced by a conducting surface can be explained by the absence of surface charge, typical for dielectric surfaces, on the central conducting electrode of the lens.

C. Long plasma lens

The plasma lens used in the investigations reported above is a short lens, with the beam focus located well outside the lens itself. Experimental studies of the possibility of long systems that would allow efficient transport of intense ion beams are of considerable interest. Note that curvilinear plasma-optical systems have been used for separation of slow plasma flows.²⁰ A long lens of length about 180 cm was used by Booth and Lefevre²² for improvement of the neutralization

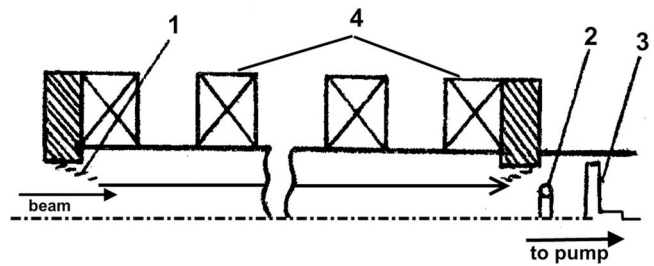


FIG. 10. Long plasma lens. 1 – lens electrodes; 2 – ring-shaped filament; 3 – collector; 4 – magnetic field system. From M. Gabovich, I. Gasanov, and I. Protsenko, *Plasma Lenses for Formation of Ion Beams* (Institute of Physics AS USSR, Kiev, 1982), Preprint # 8. Copyright 1982 by Institute of Physics NAS of Ukraine. Reprinted with permission of Institute of Physics NAS of Ukraine.

and transport of a modulated proton beam with energy about 450 keV and current about 40 mA.

Transport of ion beams by a long lens (Fig. 10) of length 70 cm and diameter 2.8 cm has been reported.²³ A uniform magnetic field was established inside the lens by means of field coils 4. The beam, after transit through a short lens, entered the long lens system located immediately after the short lens, and the exiting beam current was monitored at collector 3. The magnetic field strength inside the long electrostatic trap was up to 1 kG; different from the short-lens system, the trap here was filled with electrons by means of an incandescent ring-shaped emitter 2 (0.2 mm diameter tungsten wire) held at ground potential. Note that for proper lens operation, lower residual gas pressure was required as compared to that in the short lens case due to the increased transit time of slow ions through the longer system.

Figure 11 shows the dependence of the collected beam current on the lens potential with the filament on ($I_{fil} = 4$ A, upper curve) and off ($I_{fil} = 0$, lower curve). The experiments show increased beam transmission by the long lens by a factor of more than 4, confirming the suitability of the lens for this purpose. The dependencies of the ion beam current transported through the lens and measured by the collector (curve 1) and the electron emission current of the ring

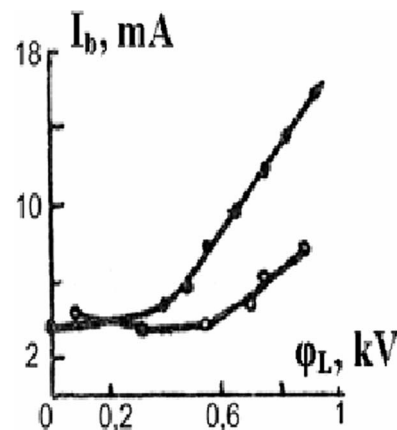


FIG. 11. Dependence of collector beam current on the lens potential. Upper curve – filament turned on ($I_{fil} = 4$ A); lower curve – turned off ($I_{fil} = 0$). From M. Gabovich, I. Gasanov, and I. Protsenko, *Plasma Lenses for Formation of Ion Beams* (Institute of Physics AS USSR, Kiev, 1982), Preprint # 8. Copyright 1982 by Institute of Physics NAS of Ukraine. Reprinted with permission of Institute of Physics NAS of Ukraine.

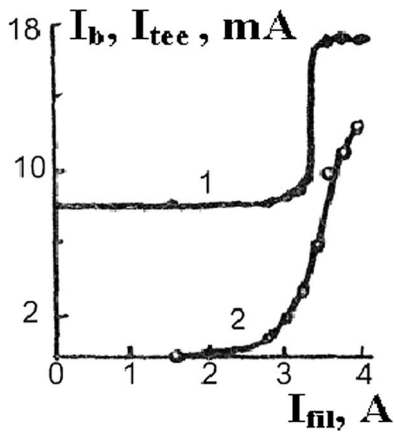


FIG. 12. Curve 1 – the collector current; 2 – electron emission current (I_{tee}). Lens potential 950 V. From M. Gabovich, I. Gasanov, and I. Protsenko, *Plasma Lenses for Formation of Ion Beams* (Institute of Physics AS USSR, Kiev, 1982), Preprint # 8. Copyright 1982 by Institute of Physics NAS of Ukraine. Reprinted with permission of Institute of Physics NAS of Ukraine.

shaped filament (curve 2) are shown in Fig. 12 (lens potential $\varphi_L = 950$ V). Figures 11 and 12 indicate that under these conditions the formation of electron space charge within the lens is more efficient using the filament than by using ion-electron emission from the electrode surfaces 1 (Fig. 10).

The experiments described in the preceding concern the focusing and transport of high-divergence intense light ion beams by short and long electrostatic plasma lenses. It has thus been demonstrated that the plasma lens can be a highly efficient strong focusing tool. The maximum ion beam current density at the focus of a short lens was up to 300 mA/cm^2 , coinciding closely with the initial ion current density of the beam at the ion source extractor, in agreement with the Langmuir formula²⁴ for maximum beam current density,

$$J_{\max} = j_o(1 + E_b/kT_i) \sin^2 \Theta, \quad (7)$$

where j_o is the initial beam current density, E_b is the beam energy, kT_i is the ion temperature (thermal energy spread), and Θ is the angle of beam focusing, $\Theta \approx R_o/F$. Factors determining the formation of strong electric fields have been studied. It has been shown that electric field formation in the plasma lens is possible with efficient generation of electrons at sufficiently low residual gas pressure. In the self-consistent mode of operation, direct contact of the beam with the ring electrode surfaces is required, together with appropriate choice of electrode configuration. Depending on the ion beam current and the electric field required for focusing, space charge overcompensation may occur in the lens. In most cases, the lens medium consists of either an almost pure electron sea for the case of low current beams as described in these experiments ($I_b/v_b \ll \varphi_L$), or a slightly charged plasma with small deviation from quasi-neutrality. In the high current regime $I_b/v_b \gg \varphi_L$.

IV. HIGH-CURRENT PLASMA LENS

Further development of the electrostatic plasma lens for the high beam current regime has been summarized in Refs. 14–17. In these experiments, we used repetitively

pulsed, broad beams 60 mm in diameter of hydrogen ions with current up to 2 A, energy up to 25 keV, and pulse duration $100 \mu\text{s}$, formed from an ion source with a three-electrode, multi-aperture extractor, entering the high-current regime for which $\varphi_L < I_b/v_b$. We have reported¹⁶ on the static and dynamic characteristics of the high-current plasma lens with quasi-neutral plasma created by fast beam ions and secondary emission electrons. Some features¹⁷ of the focusing of wide-aperture, low-divergence beams of hydrogen ions were investigated. In these experiments, good agreement was found with plasma-based optical principles. It was theoretically predicted that a lens without spherical aberrations can be obtained by using an optimum magnetic field configuration and selection of the optimum distribution of externally applied ring-electrode potentials, and optimization of the number of ring electrodes and their dimensions. These experiments confirmed good operation of the electrostatic plasma lens and a high degree of predictability, but the maximum beam compression (ratio of focused to unfocused ion beam current density at the focal spot) was limited to disappointingly low values of 2–5. It became clear²⁵ that this limitation in beam compression was connected primarily to non-removable momentum aberrations due to the azimuthal rotation of beam particles in the lens magnetic field. These aberrations depend on the ion charge-to-mass ratio through the beam velocity v_b and restrict the minimum radius of the beam at the focus to

$$R_{\min} = R_0 \cdot \frac{v_b B L}{\varphi_b \pi c}, \quad (8)$$

where R_0 is the initial radius of the beam. Beams of protons with energy 10–25 keV and low-energy singly charged copper ion beams with energy 200–400 eV were focused to a radius $R_{\min} \sim 1$ cm, for typical lens parameters ($B \sim 1$ kG). In experiments with multiply charged metal ion beams (Cu, Zn, Mo) formed by a vacuum arc ion source with energies 100–400 eV it was demonstrated that the lens gave rise to charge-state separation of particles at the focus. For higher energy heavy ions the effect of momentum aberrations is much reduced and the electrostatic plasma lens can be a very effective tool for focusing large area, high current, energetic heavy-ion beams, as has been well demonstrated in a number of experimental investigations performed at Kiev^{25,26} (IP NASU) and at Berkeley (LBNL).^{27,28} A 20–30 keV copper ion beam was brought to a focal spot of size $R_{\min} \sim 1$ mm, for example.

The experimental arrangements used at Kiev²⁶ and at Berkeley^{27,28} have been described. The lens used in these experiments employed a magnetic field that was established by conventional current-driven electromagnetic coils. A vacuum arc ion source was used for beam production,²⁹ operating in a repetitively pulsed mode and producing a low-divergence beam with parameters: Kiev – pulse duration $100 \mu\text{s}$, beam extraction voltage up to 25 kV, total beam current up to 0.8 A, initial beam diameter 5.6 cm, ion species C and Cu; Berkeley – pulse duration $250 \mu\text{s}$, beam extraction voltage up to 50 kV, beam current up to 0.5 A, initial beam diameter 10 cm, beam species C, Cu, Zn, Ta, Pb, Bi. The basic parameters of the lens were: Kiev – input aperture 7 cm, length 12 cm, number of ring electrodes 9, maximum potential applied to the central electrode +4.7 kV; Berkeley – aperture 10 cm, length 20 cm,

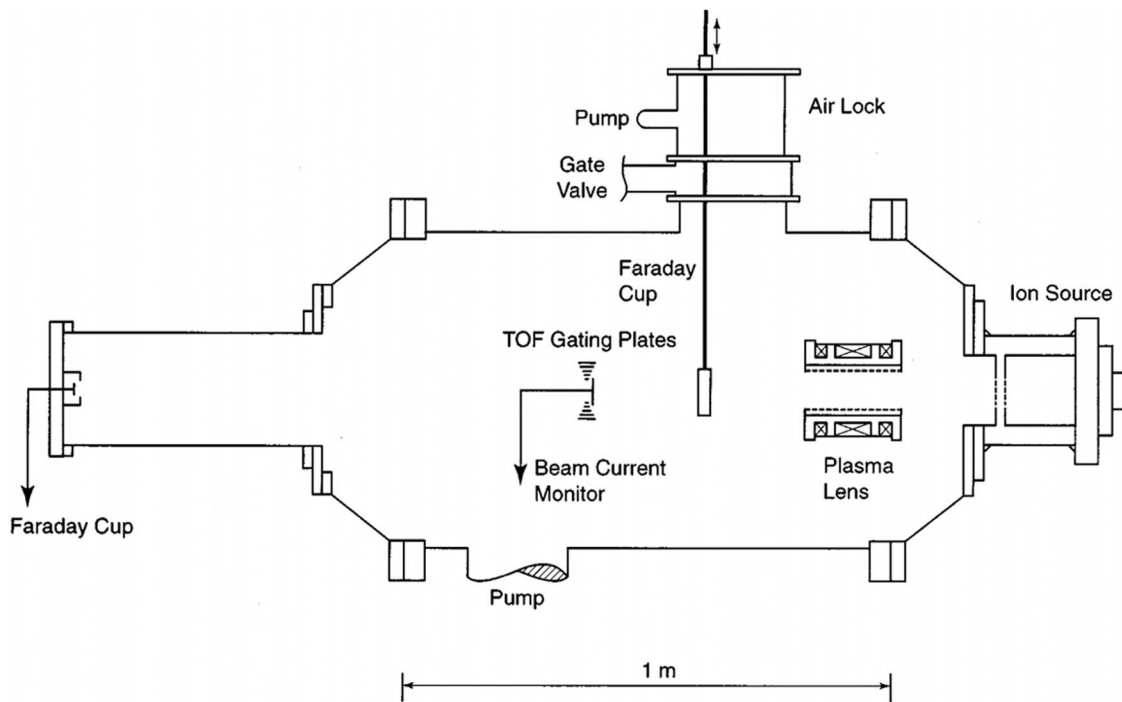


FIG. 13. Simplified schematic of the experimental configuration used at Berkeley. Reprinted with permission from Appl. Phys. Lett. **75**, 911 (1999). Copyright 1999 American Institute of Physics.

number of ring electrodes 9, lens potential +10 kV. A pulsed magnetic field of magnitude up to 0.1 T and pulse width up to 500 μs was established by small solenoid coils surrounding the lens. Movable Langmuir and capacitive probes were used for measurements of the plasma characteristics. The residual pressure was less than 1×10^{-5} Torr. A low temperature plasma was formed in the lens volume by the ion beam itself through secondary electron emission from the lens electrodes. Note that ionization of the background gas by the beam is not a significant effect at the operating pressure and beam pulse length employed.

The Kiev experiments²⁶ were first targeted at modeling the conditions needed for carrying out high-dose metal ion implantation at moderate energies (10–100 keV). For the beams used here, the value of the beam potential parameter I_b/v_b is comparable to the beam energy, and high current beams such as these can exist only in the fully compensated state (i.e., fully space-charge neutralized), with the cold electron background produced, for example, by secondary emission from surrounding metal surfaces. Our experiments showed²⁶ that this leads to a sharp increase in electron current flow from the background plasma to the lens electrodes by about an order of magnitude compared to the case of a hydrogen ion beam. Operation of the lens with a resistive voltage divider to supply the ring electrode voltages is then not reasonably possible because of the high currents involved, and we used instead an RC-divider which was able to hold the electrode voltages constant throughout the beam pulse. For conditions optimized for minimum spherical aberrations, we showed that the maximum current density of copper ions onto a target at the focus was about 170 mA/cm², corresponding to a compression at the focus of a factor of about 20.

Further experiments were performed at Berkeley.^{27,28} The experiments explored operation of the lens with moderate energy, high current, large area, heavy metal ion beams. The midplane of the plasma lens was located 34 cm from the ion source extractor. The lens electrodes were fed through a 110 k Ω voltage divider by a low-impedance stabilized power supply. The highest potential $\phi_L \leq +10$ kV was on the central lens electrode, and the remaining symmetrically disposed electrodes were connected in pairs to the appropriate voltage divider points. The power supply provided fixed voltages to the lens electrodes during transport of the beam through the lens. The beam current density was measured by a radially movable, magnetically suppressed Faraday cup located a further 34 cm downstream from the lens midplane; the entrance aperture of the Faraday cup was 1 cm diameter for most of the work but we reduced this to 3 mm diameter for some measurements so as to obtain greater spatial (radial) resolution. The total ion beam current was measured by scanning the Faraday cup radially and integrating the radial beam profile. We could also monitor the total current by a simple collector plate without suppression of secondary electrons. A time-of-flight ion charge state analysis system³⁰ was used to monitor the ion charge state spectrum of the beam transported through the lens. A simplified schematic of the experimental configuration is shown in Fig. 13.

Experiments have shown, in prior work as well as in the work described here, that the plasma lens focusing characteristics depend strongly on the externally applied potential distribution along the electrostatic ring electrodes. Variation of the electrode potential distribution can change the lens operating regime from focusing to defocusing. The effect of spherical aberrations is minimized when the lens electrode

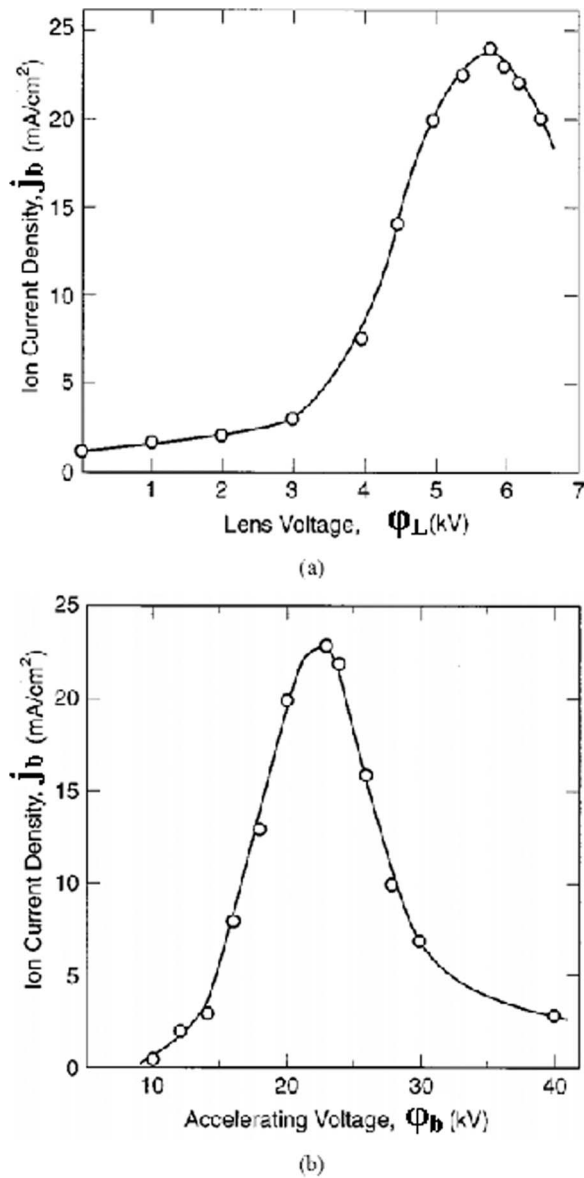


FIG. 14. Tantalum ion beam current density j_b at the Faraday cup for optimum potential distribution: (a) as a function of lens central electrode voltage φ_L ; $\varphi_b = 22$ kV, $B = 800$ G and (b) as a function of beam accelerating voltage φ_b ; $\varphi_L = 5.5$ kV, $B = 800$ G. Reprinted with permission from Appl. Phys. Lett. **75**, 911 (1999). Copyright 1999 American Institute of Physics.

potentials are optimally distributed, which occurs when the potential variation follows the magnetic field variation, $\Phi(R, z) \sim B(0, z)$ as follows from theoretical considerations (see Eq. (5)). Then the dependencies $j_i(\varphi_L, \varphi_b)$ have a distinct sharply peaked character, see Fig. 14, and maximum beam compression is observed at the focus.

The plasma lens can be used as a focusing tool for creation of a spot with high energy density at the focus. Good beam focusing under optimum conditions was visually observed in the form of a bright spot of overall diameter 2–3 cm at the Faraday cup location; the tantalum ion beam compression was a factor of more than $30\times$.

We consider now some possible factors limiting the maximum compression of the focused beam. Momentum aberrations, finite phase volume, and incomplete space charge com-

ensation of the beam at the focus were taken into consideration. As shown above, momentum aberrations can restrict the focused beam compression to a factor of 1000 or less. Using some equations from Ref. 17 (the Langmuir formula, Eq. (7) for this case can be rewritten as $j_{\max} \leq j_0 \frac{R_0^2}{F^2} \cdot \frac{E_b}{T_{i0}}$ because of finite phase volume of the beam, where T_{i0} is the temperature of ions in within the source, E_b is the beam energy, and F is the focal length) and

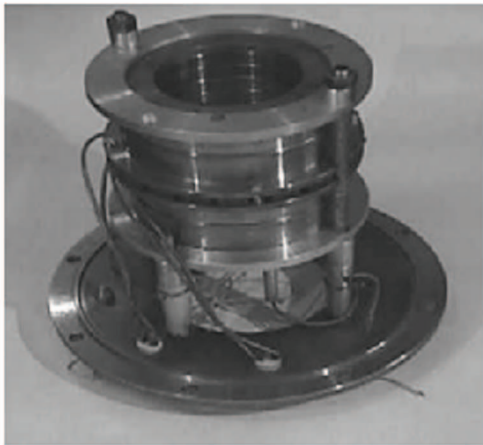
$$j_{\max} \leq j_0 \exp \left[\frac{R_0^2}{F^2} \cdot \frac{mv_b^2}{2eQ} \cdot \frac{1}{\alpha I_b / v_b} \right], \quad (9)$$

due to incomplete compensation of the beam at the focus (where α is the beam space charge compensation factor, $\alpha = 1 - n_e / Qn_b$), it can be shown that for the experimental conditions ($\varphi_b = 30$ kV, $\varphi_L = 6$ kV, $R_0 = 5$ cm) both these mechanisms may limit the beam compression to a factor of up to 1000. Here, we take $T_{i0} \leq 4$ eV, and the radial potential drop across the focused beam according to measurements from Ref. 17 is $\alpha \cdot I_b / v_b \sim 100\text{--}200$ V. These factors can occur for beam compression about 1000 under these conditions. We can conclude that the maximum beam compression observed experimentally is not restricted by removable spherical aberrations because of the finite width of the lens electrodes. This was well confirmed by computer simulation of processes of formation of the plasma within the lens volume under conditions close to experimental.³⁵ Note that the presence of spherical aberrations may play a beneficial role — as the lens ring-electrode potentials are adjusted one can tailor the beam radial profile at the collector and thus create a uniform current density distribution. This has been shown experimentally and theoretically in Ref. 17.

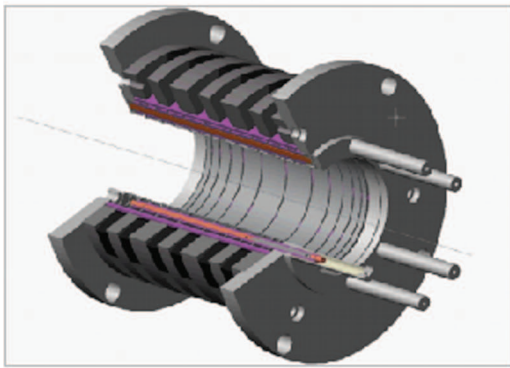
V. PERMANENT MAGNET PLASMA LENS

In the experiments described above we noted a significant increase in the focused ion beam current density for specific low magnetic field strengths, suggesting the possibility of a plasma lens using permanent magnets. The first such experiments using permanent magnets to establish the magnetic field configuration were carried out collaboratively between the IP NASU (Kiev) and LBNL (Berkeley).^{31–34}

The parameters of the lenses used with permanent magnets were as follows. Kiev: input aperture $D = 7.4$ cm, length $L = 14$ cm, number of ring-electrodes $N = 13$; maximum strength of the magnetic field formed by the small Fe-Nd-B magnets at the center of the lens was $B = 360$ G. Berkeley: $D = 10$ cm, $L = 15$ cm, $N = 11$; $B = 300$ G. The magnetic field shape required for each plasma lens was determined by computer simulation and experimental tests; the simulation results were in excellent agreement with the experimental data. Radially movable Langmuir probes were used for measurement of the plasma in the lens volume and in the beam drift space. I_b and J_b were measured by an axially movable sectioned collector (at Kiev) and by a radially movable, magnetically suppressed Faraday cup with entrance aperture 3 mm (at Berkeley), located at a distance ~ 30 cm from the lens mid-plane. The base pressure in the vacuum chamber was less than 1×10^{-5} Torr, allowing formation of plasma within the lens



(a)



(b)

FIG. 15. Electrostatic plasma lens using permanent magnets. Input aperture 10 cm, length 15 cm, number of cylindrical electrodes 11; magnetic field strength formed by the Fe-Nd-B permanent magnets 300 G. (a) General view; (b) cut-away view. Reprinted with permission from A. A. Goncharov and I. G. Brown, *IEEE Trans. Plasma Sci.* **35**, 986 (2007). Copyright 2007 Institute of Electrical and Electronics Engineers, Inc.

volume by the ion beam itself and by secondary electron emission from the lens electrodes. The embodiment of plasma lens used at LBNL is shown in Fig. 15.

The characteristics and focusing properties of these lenses were explored as a function of externally applied electrode potential distribution, magnetic field strength, and manner of establishing the magnetic field (i.e., solenoid or permanent magnets), total ion beam current transported, initial beam diameter, and ion species. The experiments confirm that the plasma lens is effective in focusing large area (up to $D = 10$ cm), high-current (up to 1 A), heavy metal ion beams with moderate energy (5–100 keV). The focusing properties of the lens are similar, under the same parametric conditions, for both the cases when the lens magnetic field is established by a current-driven solenoid and with a permanent magnet array.

The experiments show that for a large-area ion beam the focusing properties are more distinct when the initial beam diameter equals the lens input aperture diameter. The maximum compression for a tantalum ion beam was a factor of 5–7 for the optimal lens potential distribution, for the case of a beam

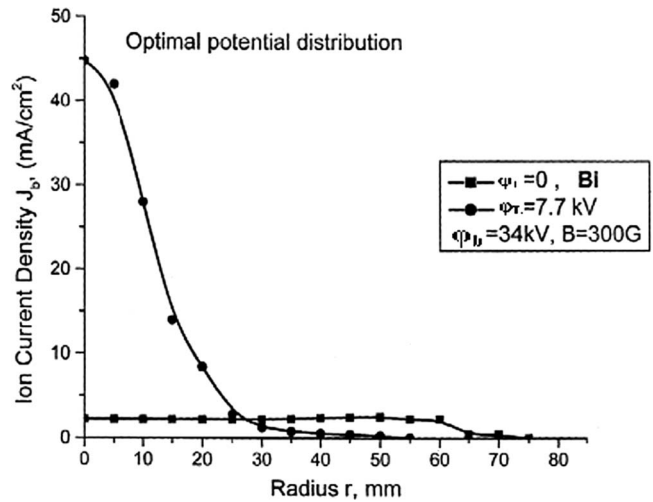


FIG. 16. Radial ion beam current density profile at the Faraday cup location. Reprinted with permission from A. A. Goncharov and I. G. Brown, *IEEE Trans. Plasma Sci.* **32**, 80 (2004). Copyright 2004 Institute of Electrical and Electronics Engineers, Inc.

with initial diameter 6 cm. For the case of a tantalum beam with diameter 10 cm, the maximum beam compression at the lens focus was approximately a factor of 30, with current density up to 32 mA/cm². Focusing of different ion beams species (C, Mg, Cu, Nb, Ta, Pb, Bi) was investigated. The best results were obtained for Bi, Pb, and Ta. In Fig. 16, one can see good bismuth beam compression for the case of optimal electrode potential distribution.

The maximum ion beam compression for Bi was up to a factor of 30–40, and the low-noise focused beam current density was up to 45 mA/cm². At the same time, the total transported ion beam current increased by up to 30%. The experimental results imply that the maximum beam compression factor is restricted by non-removable spherical aberrations because of the finite width of the lens electrodes. Oscilloscopes showing the ion beam current collected by the on-axis Faraday cup for the lens on, and with the optimal potential distribution, compared to the case with lens off, are shown in Fig. 17. Importantly, note that the pulse shape of the focused beam follows the initial beam pulse shape. That is, under these conditions the lens neither distorts the focused beam pulse-shape nor introduces any additional beam noise.

These experimental results were used for theoretical analysis and computer simulation of the plasma formation processes within the lens volume (see Fig. 15).^{35,36} Some of these results are shown in Figs. 18 and 19 (see Refs. 35 and 36 for more detail). These data show clearly the formation within the lens of layered electron structures (Fig. 18) due to the finite width of the ring-electrodes. This means that the presence of spherical aberrations restricts the maximum compression of the focused ion beam. This is confirmed in Fig. 19, which models the ion beam focusing for the experimental conditions used. The maximum compression obtained by computer simulation is in good accordance with experimental results.

There is yet another important factor that can degrade the ion beam focusing. This is connected with a drift

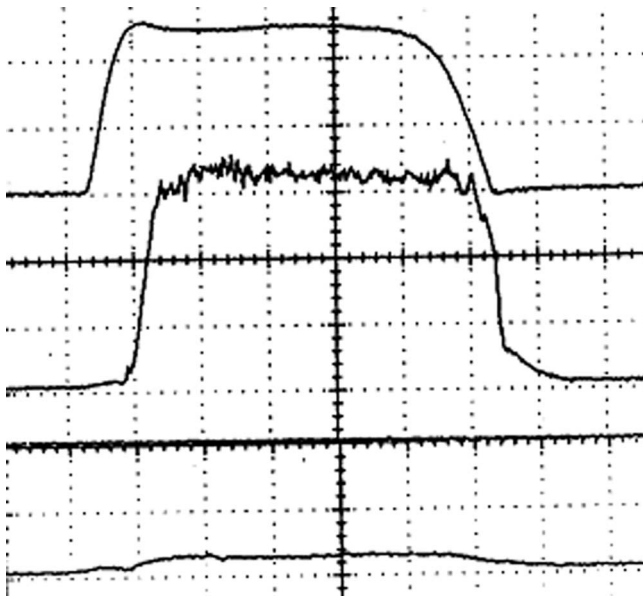


FIG. 17. Oscillograms of the beam current (in “average” mode) at the on-axis Faraday cup, for the case of maximum current compression and when the lens electrode potential distribution is optimum. Beam accelerating voltage $\varphi_b = 34$ kV, $\varphi_L = 7.7$ kV, $B = 300$ G. Upper trace: ion source arc current (200 A/cm). Vertical scale 14 mA/cm for both middle (plasma lens on) and lower (plasma lens off) traces; horizontal scale $50 \mu\text{s/cm}$ sweep speed. Reprinted with permission from Appl. Phys. Lett. 75, 911 (1999). Copyright 1999 American Institute of Physics.

instability arising in inhomogeneous crossed $\mathbf{E} \perp \mathbf{B}$ fields in the lens volume due to the inherent non-removable radial gradient of magnetic field. These collective processes were first observed in experiments described in Ref. 16. When a hydrogen ion beam was transported through the lens, small-scale turbulent oscillations arise in the 20–50 MHz frequency range. A linear dispersion equation for two-dimensional oscillations was obtained that allowed us to explain qualitatively the regularities observed in the experiments. Further understanding of the instability mechanisms requires studying the nonlinear dynamics of electrons within the plasma lens medium. A nonlinear equation for the perturbation electric potential has been obtained,^{37,39} describing the dynamics

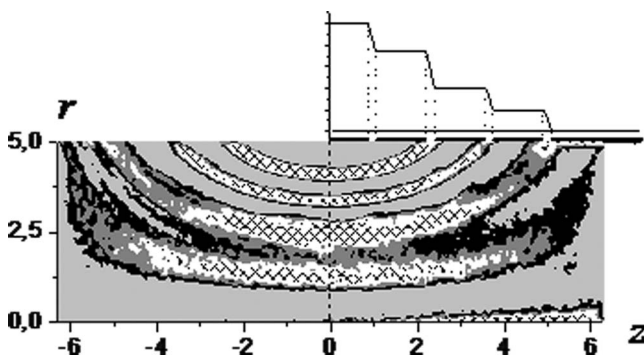


FIG. 18. Electron space charge distribution in the plasma lens volume for the optimal lens potential distribution. The background ion space charge is 0.43 CGSE units/cm³. Shaded areas – electron space charge density ($Q_e \geq 0.86$ CGSE units/cm³). (Units of r and z axes are cm). Reprinted with permission from Rev. Sci. Instrum. 75, 1662 (2004). Copyright 2004 American Institute of Physics.

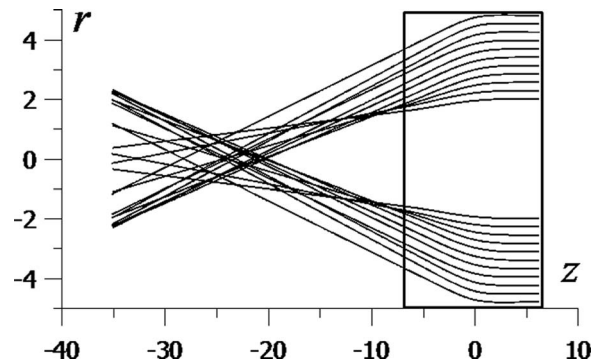


FIG. 19. Ion beam particle trajectories for the case of Fig. 18. (Units of r and z axes are cm). Reprinted with permission from Rev. Sci. Instrum. 75, 1662 (2004). Copyright 2004 American Institute of Physics.

of the generation and evolution of electron wave vortex-like structures within the lens. This equation describes the development of both large scale, low frequency, vortex structures and small scale, high frequency vortices. Using heavy ion beams we could distinguish regular low frequency (0.2–2 MHz) electrostatic potential waves rotating around the lens axis, and irregular small scale noise in the 20–50 MHz range.^{16,32,38,42} These results are in good accordance with theoretical analysis of the excitation and evolution of electron vortex-like structures in the high current plasma lens.^{37–39}

It was noted that the ion beam noise (beam current fluctuation level) inherent to the vacuum arc ion source can be enhanced when the beam passes through a region of the lens volume. We found experimentally that there is a very narrow range of low magnetic fields, with $\rho_e \leq R$ (where ρ_e is the electron Larmor radius and R is the lens radius), for which the focusing properties of the lens improve dramatically. At the same time, in this range the turbulence level in the lens volume and in the focused ion beam decrease by more than an order of magnitude (Fig. 20). Under these conditions the maximum beam compression significantly exceeds that obtained for typical lens magnetic fields. Note also that computer simulation results indicate that in this case spherical aberrations in main lens volume can be eliminated.

The simple design, flexibility, robust construction, the need for only a single power supply, and the high efficiency are all attractive advantages of a lens using permanent magnets rather than current-driven coils. The use of small permanent magnets for establishing the required magnetic field configuration provides the possibility for development of a new generation of plasma lenses. Such advanced, improved, and cost effective lenses with low noise and minimal spherical aberrations could be used in the low energy injection beam lines of heavy ion linear accelerators, for example, between the ion source and the RFQ pre-accelerator system where there exists a severe concern of beam space-charge blow-up. There remains, however, one very important factor that could restrict the use of the plasma lens for accelerator applications, namely, the possibility of a negative influence of the lens on the emittance of the ion beam due to inherent lens noise and aberrations.

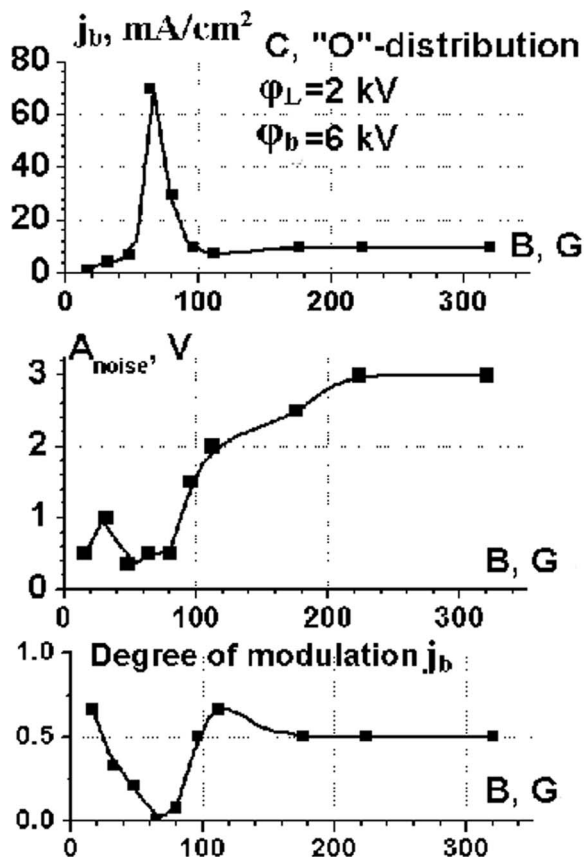


FIG. 20. Characteristics of plasma lens in the low magnetic field regime. (Upper) ion current density at collector as a function of lens magnetic field strength. (Middle) capacitive probe signal (noise amplitude) within the lens volume as a function of lens magnetic field. (Lower) amplitude of modulation in ion current density (noise amplitude) as a function of lens magnetic field. Reprinted with permission from Rev. Sci. Instrum. **75**, 1662 (2004). Copyright 2004 American Institute of Physics.

VI. EFFECT OF PLASMA LENS ON ION BEAM EMITTANCE

In the work described in Refs. 40 and 41, we carried out measurements of the emittance of a high current, moderate energy ion beam following its transport through a permanent-magnet electrostatic plasma lens. We used an advanced plasma lens with minimized magnetic field gradients in the range of low magnetic fields for which $\rho_e \approx R$ (where ρ_e is the electron Larmor radius and R is the typical lens dimension). According to Eq. (5), this should significantly decrease the influence of spherical aberrations (the second term in Eq. (5) disappears). A simplified schematic of the lens with its improved magnetic field configuration is shown in Fig. 21. This plasma lens has a 13-electrode system with 74 mm input aperture and 16 cm length. A maximum voltage ϕ_L of up to +4.7 kV (dc or pulsed) was applied to the central electrode. The lens magnetic field was formed by Fe-Nd-B permanent magnets, and at the center of the lens $B = 126$ G. The magnetic field configuration was determined by numerical calculations to minimize magnetic field gradients. In Fig. 22, one can see that the radial gradient of magnetic field is very small, and the range of the uniform magnetic field in the axial direction is extended.

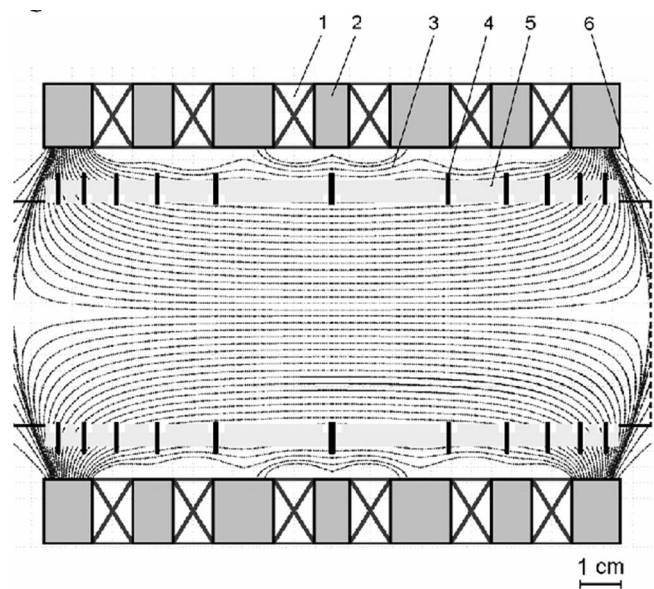


FIG. 21. Plasma lens with minimized magnetic field gradients. 1 – permanent magnets; 2 – magnetic conductor; 3 – magnetic field lines; 4 – electrodes; 5 – interelectrode insulating spacers; 6 – metal grid. Reprinted with permission from A. A. Goncharov and I. G. Brown, IEEE Trans. Plasma Sci. **35**, 986 (2007).

The results of our explorations show that the emittance of the high current ion beam does not grow due to the lens, when the lens is adjusted for optimal beam focusing (implying also suppression of noise and removal of spherical aberrations). The emittance measured by a “pepper pot” technique for a 16 keV, 250 mA, Cu ion beam produced by a vacuum arc ion source was about 0.6π mm mrad at a beam current of 50 mA,

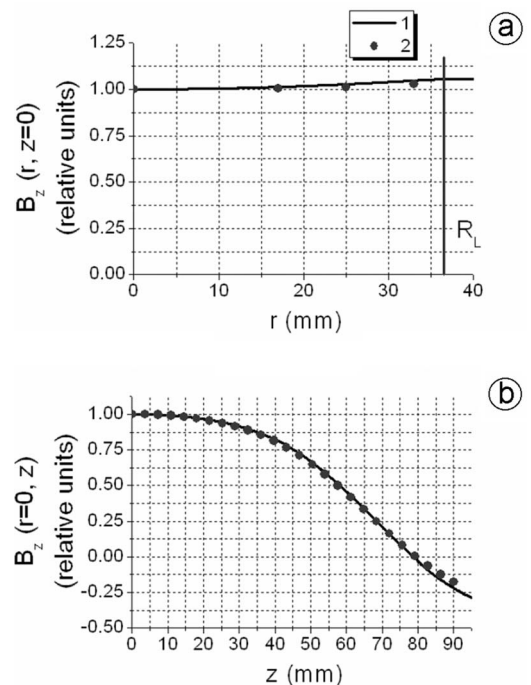


FIG. 22. Radial and axial distribution of magnetic field in the lens; 1 – calculated distribution; 2 – measured distribution. Reprinted with permission from A. A. Goncharov and I. G. Brown, IEEE Trans. Plasma Sci. **35**, 986 (2007).

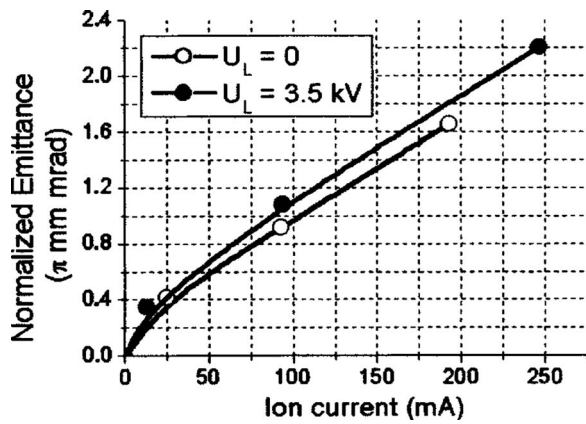


FIG. 23. Dependencies of the normalized emittance on ion beam current, with the lens turned off and on. Reprinted with permission from Appl. Phys. Lett. **86**, 041502 (2005). Copyright 2005 American Institute of Physics.

increasing more-or-less linearly to 2.2π mm mrad at 250 mA, and was conserved during beam transport through the lens (Fig. 23). We see that for these experimental conditions the lens has no significant influence on the ion beam emittance over a wide range of beam current.

Another important result was that the absolute value of the emittance was found to be much greater than anticipated. This discrepancy is likely a result of the multi-aperture ion optic system (ion source extractor) and by the fact that the divergence of the ion beam is mainly due to non-thermal effects.

VII. FACTORS RESTRICTING THE MAXIMUM COMPRESSION OF WIDE-APERTURE INTENSE ION BEAMS FOCUSED BY THE PLASMA LENS

As has been shown in Ref. 17 and mentioned above, the maximum compression factor for wide aperture, low divergence, heavy ion beams focused by the plasma lens can be limited by lens static and dynamic aberrations, non-compensated space charge, and final phase volume of the focused beam. Using a plasma lens with small radial magnetic field gradients in the low magnetic field regime,⁴⁰ we could greatly reduce the noise and spherical aberrations and also the influence of space charge. As a result, we obtained a maximum compression factor for optimum lens operation of 30–40, as we had obtained previously in a number of experiments. Taking into consideration the actual experimental value of emittance of the focused ion beam, we believe that these results indicate that the maximum compression factor is limited primarily by the beam emittance as determined by the ion source beam formation electrodes. Similarly, the focusing of single-aperture, high-divergence, high-brightness ion beams can be restricted by the maximum initial beam density at the extraction hole according to the Langmuir formula.

In order to focus properly, neutralization of the medium in the lens volume is required. The neutralization process takes some time due to finite electron mobility and other factors, and this feature can lead to restrictions on the simple and straightforward application of the plasma lens for the focusing of very short pulse ion beams.

VIII. CONCLUSION

We have summarized work carried out over more than half a century on the electrostatic plasma lens based on the plasma optical principles of magnetic electron isolation and equipotentialization along magnetic field lines. Many attractive possibilities for focusing and manipulating high current energetic positive heavy ion beams have been demonstrated. At the current level of investigation, these plasma optical tools could find effective and relatively low cost application in the low energy beam lines of heavy linear accelerators between the ion source system and the accelerator entrance. Application for high-dose ion implantation has also been demonstrated.⁴³ Further development of plasma lenses could be connected to applications for focusing short-pulse, high-energy, high-brightness, intense ion beams in heavy ion fusion experiments.⁴⁴ This may require further experimental and theoretical research for creating the optimal plasma medium within the lens volume for very short pulse ion beams for which the pulse duration is comparable to or less than the time for electron compensation.

The plasma lens configuration involving crossed E and B fields and the particular ion-electron plasma medium, leads to very convenient conditions for exploration of fundamental phenomena of collective processes due to interaction of the propagating ion beam with magnetized electrons, leading to the appearance of electron vortex structures. For example, the generation of large scale electron vortices in the plasma lens volume has been experimentally observed.⁴²

The plasma lens configuration provides an attractive method for establishing a stable plasma discharge at low pressure.^{45,46} Use of the lens configuration in this way has been applied for low cost, low maintenance, high reliability plasma generation devices using permanent magnets for ion cleaning, activation and polishing of substrates directly before deposition, and for sputtering. They can operate separately and in a single processing cycle with a sputtering system.

We point out that these devices^{46,47} can also operate with a positive space charge cloud, and thereby find application for focusing and manipulating intense negative ion beams and electron beams. The focusing of laser produced plasma may also be a new field of application.⁴⁸

ACKNOWLEDGMENTS

The author would like to thank Dr. Ian Brown (LBNL) for fruitful and stimulating discussion, comments, and valuable support in preparing this paper, and Dr. Igor Kaganovitch (PPPL) for his encouragement.

¹J. Koch, *Electromagnetic Isotope Separators and Applications of Electromagnetically Enriched Isotopes* (North Holland, Amsterdam, 1958).

²A. J. T. Holmes, in *The Physics and Technology of Ion Sources*, edited by I. G. Brown (Wiley, New York, 1989), p. 53.

³W. K. H. Panofsky and W. R. Baker, *Rev. Sci. Instrum.* **21**, 445 (1950).

⁴F. Winterberg, *Z. Naturforsch.* **32a**, 840 (1977).

⁵P. F. Ottinger, D. Mosher, and S. A. Goldstein, *Phys. Fluids* **22**, 332 (1979).

⁶P. F. Ottinger, D. Mosher, and S. A. Goldstein, *Phys. Fluids* **23**, 909 (1980).

⁷M. D. Gabovich, A. A. Goncharov, I. M. Protsenko, and S. V. Kharitonov, in *Proceedings of the XIIIth International Conference on Ionized Gases, Berlin, 1977* (Physical Society of the GDR, Berlin, 1977), p. 919; See also

- A. A. Goncharov, I. M. Protsenko, and V. V. Tsiolko, *Zh. Tech. Fiz.* **50**(12), 2556 (1980).
- ⁸A. I. Morozov, *Dokl. Acad. Nauk. USSR* **163**(6), 1363 (1965).
- ⁹A. I. Morozov, *Introduction to Plasmadynamics* (Fismatlit, Moscow, 2008), p. 572.
- ¹⁰A. I. Morozov and S. Lebedev, in *Reviews of Plasma Physics*, edited by M. Leontovich (Consultants Bureau, New York, 1975), p. 247.
- ¹¹D. Gabor, *Nature (London)* **160**, 89 (1947).
- ¹²O. Meusel, A. Bechtold, J. Pozimski, U. Ratzinger, A. Schempp, and H. Klein, in *Proceedings of LINAC 2004, Lübeck, Germany* (World Scientific, 2004), pp. 465–467.
- ¹³K. Schulte, M. Droba, B. Glaeser, S. Klapproth, O. Meusel, and U. Ratzinger, in *Proceedings of IPAC2012, New Orleans, LA* (Institute of Electrical and Electronics Engineers, Inc., 2012), pp. 1164–1166.
- ¹⁴A. A. Goncharov, A. Zatuagan, and I. Protsenko, *Pis'ma Zh. Tekh. Fiz.* **15**(6), 1 (1989).
- ¹⁵A. Goncharov, *Rev. Sci. Instrum.* **69**, 1150 (1998).
- ¹⁶A. A. Goncharov, A. N. Dobrovolsky, A. V. Zatuagan, and I. M. Protsenko, *IEEE Trans. Plasma Sci.* **21**, 573 (1993).
- ¹⁷A. A. Goncharov, A. V. Zatuagan, and I. M. Protsenko, *IEEE Trans. Plasma Sci.* **21**, 578 (1993).
- ¹⁸V. Zhykov, A. Morozov, and G. Schepkin, *JETP Lett.* **9**(1), 24 (1969); See also A. I. Morozov, “Plasmadynamics,” in *Encyclopedia of Low-Temperature Plasma*, edited by V. E. Fortov (Springer, 2008), Vol. 46.
- ¹⁹M. Gabovich, I. Gasanov, and I. Protsenko, *Pis'ma Zh. Tekh. Fiz.* **3**(21), 1153 (1977); See also M. Gabovich, I. Gasanov, and I. Protsenko, *Plasma Lenses for Formation of Ion Beams* (Institute of Physics AS USSR, Kiev, 1982), Preprint # 8.
- ²⁰I. Aksenov, V. Padalka, and V. Khoroshikh, *Plasma Phys. Rep.* **6**(2), 312 (1980).
- ²¹S. Robertson, *Phys. Rev. Lett.* **48**, 149 (1982).
- ²²R. Booth and H. W. Lefevre, *Nucl. Instrum. Methods* **151**, 143 (1978).
- ²³A. Goncharov and I. Protsenko, *Ukr. Phys. J.* **6**(11), 1659 (1991).
- ²⁴M. D. Gabovich, *Physics and Techniques of Plasma Ion Sources* (Atomisdat, Moscow, 1972), p. 247; See also J. R. Pierce, *Theory and Designs of Electron Beams* (Van Nostrand, New York, 1954).
- ²⁵A. Goncharov, A. Dobrovolsky, I. Litovko, I. Protsenko, and V. Zadorodny, *IEEE Trans. Plasma Sci.* **25**, 709 (1997).
- ²⁶A. Goncharov, A. Dobrovolsky, I. Protsenko, V. Kaluh, I. Onishchenko, and I. Brown, *Rev. Sci. Instrum.* **69**, 1135 (1998).
- ²⁷A. Goncharov, I. Protsenko, G. Yushkov, and I. Brown, *Appl. Phys. Lett.* **75**, 911 (1999).
- ²⁸A. Goncharov, I. Protsenko, G. Yushkov, and I. Brown, *IEEE Trans. Plasma Sci.* **28**, 2238 (2000).
- ²⁹I. G. Brown, *Rev. Sci. Instrum.* **65**, 3061 (1994); See also *The Physics and Technology of Ion Sources*, edited by I. G. Brown (Wiley, New York, 1989), pp. 257–284.
- ³⁰I. G. Brown, J. E. Galvin, R. A. MacGill, and R. T. Wright, *Rev. Sci. Instrum.* **58**, 1589 (1987).
- ³¹A. Goncharov, *Rev. Sci. Instrum.* **73**, 1004 (2002).
- ³²A. Goncharov, V. Gorshkov, S. Gubarev, A. Dobrovolsky, I. Protsenko, and I. Brown, *Rev. Sci. Instrum.* **73**, 1001 (2002).
- ³³I. Protsenko, A. Goncharov, V. Gorshkov, S. Gubarev, I. Litovko, and I. Brown, in *Proceedings of the XXth International Symposium on Discharges and Electrical Insulation in Vacuum (ISDEIV), Tours (France)* (IEEE, 2002), p. 287.
- ³⁴A. A. Goncharov and I. G. Brown, *IEEE Trans. Plasma Sci.* **32**, 80 (2004).
- ³⁵V. Gorshkov, A. Goncharov, and A. Zavalov, *Plasma Phys. Rep.* **29**, 874 (2003).
- ³⁶A. Goncharov, V. Gorshkov, V. Maslov, V. Zadorozhny, and I. Brown, *Rev. Sci. Instrum.* **75**, 1662 (2004).
- ³⁷A. Goncharov and I. Litovko, *IEEE Trans. Plasma Sci.* **27**, 1073 (1999).
- ³⁸A. Goncharov, S. Gubarev, V. Maslov, and I. Onishchenko, *Prob. At. Sci. Technol.* **3**, 152 (2001).
- ³⁹A. Goncharov, V. Maslov, and I. Onishchenko, *Plasma Phys. Rep.* **30**, 662 (2004).
- ⁴⁰Yu. Chekh, A. Goncharov, I. Protsenko, and I. Brown, *Appl. Phys. Lett.* **86**, 041502 (2005).
- ⁴¹Yu. Chekh, A. Dobrovolsky, A. Goncharov, I. Protsenko, and I. Brown, *Nucl. Instrum. Methods Phys. Res. B* **243**, 227 (2006).
- ⁴²Yu. Chekh, A. Goncharov, and I. Protsenko, *Tech. Phys. Lett.* **32**(1), 51 (2006).
- ⁴³A. Goncharov, I. Protsenko, G. Yushkov, O. Monteiro, and I. Brown, *Surf. Coat. Technol.* **128–129**, 15 (2000).
- ⁴⁴I. D. Kaganovich, R. C. Davidson, M. A. Dorf, E. A. Startsev, A. B. Sefkow, E. P. Lee, and A. Friedman, *Phys. Plasma* **17**, 056703 (2010).
- ⁴⁵A. A. Goncharov and I. G. Brown, *IEEE Trans. Plasma Sci.* **35**, 986 (2007).
- ⁴⁶A. Dobrovolskiy, S. Dunets, A. Evsyukov, A. Goncharov, V. Gushenets, I. Litovko, and E. Oks, *Rev. Sci. Instrum.* **81**, 02B704 (2010).
- ⁴⁷A. A. Goncharov, A. N. Dobrovolsky, S. N. Dunets, I. V. Litovko, V. I. Gushenets, and E. M. Oks, *Rev. Sci. Instrum.* **83**, 02B723 (2012).
- ⁴⁸C. Pagano, A. A. Goncharov, and J. G. Lunney, *Rev. Sci. Instrum.* **83**, 02B701 (2012).